

# A Study on Analysis of Dynamic Characteristics and Evaluation of Dynamic Compliance of a 5-Axis Multi-tasking Machine Tool by Using F.E.M and Exciter Test

Sung-Hyun Jang\*, Young-Hyu Choi<sup>+</sup>, Jong-Sik Ha<sup>++</sup>

(논문접수일 2008. 10. 16, 심사완료일 2009. 1. 19)

유한요소법과 가진시험법을 이용한 다기능 5축 복합가공기의 동특성 해석 및  
동적 컴플라이언스 평가에 관한 연구

장성현\*, 최영휴<sup>+</sup>, 하중식<sup>++</sup>

## Abstract

This paper describes a study on dynamic characteristics analysis and dynamic compliance evaluation of a 5-axis multi-tasking machine tool of ram-head type. Structural dynamics analysis and evaluation are necessary to machine tool design and development to secure good machine tool performance against tough and harsh machining conditions. In this study, natural frequencies and corresponding vibration modes of the machine tool structure were analyzed by using both F.E.M. modal analysis and impulse hammer test. Furthermore, dynamic compliance of the machine tool was analyzed by using F.E.M. and also measured by using a hydraulic exciter test. Both the theoretical analysis and experimental test results showed good agreement with each other.

**Key Words** : 5-axis multi-tasking machine(다기능 5축 복합가공기), Ram head module(램 헤드 모듈), Dynamic compliance (동적 컴플라이언스), Exciter test(가진시험법), Impulse hammer(충격망치)

\* 창원대학교 기계설계공학과

+ 교신저자, 창원대학교 매킨로닉스공학부 (yhchoi@changwon.ac.kr)

주소: 641-773 경남 창원시 사람동 9

++ 한국정밀기계(주)

## 1. Introduction

Recently, simultaneous 5-axis and multi-task machining are increasingly in demand for large scale products, such as ship propeller, crank shaft of marine engine, and so on. Multi-tasking machine tool (MTMT) is efficient and beneficial because it has various machining functions,

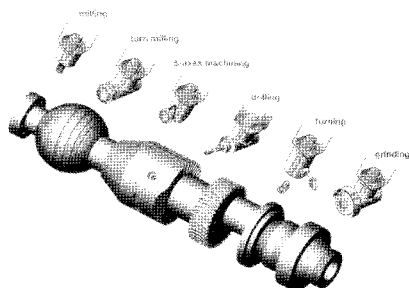
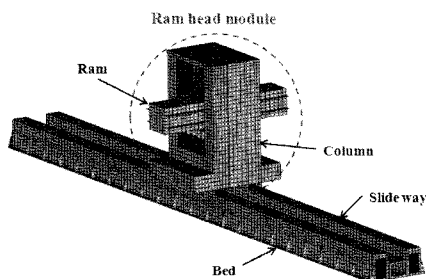
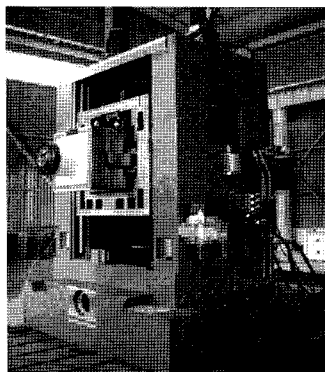


Fig. 1 Typical machining functions of a MTMT for machining a crank shaft



(a) Illustration of the full MTMT structure



(b) Ram head module

Fig. 2 A 5-axis multi-tasking machine tool

such as milling, drilling, turning, grinding, as shown in Fig. 1, all together at one machine. It can do 5-face machining and multi-task machining with just single set-up.

However, MTMT may inherently experience severe vibrations during its operations due to complex cutting forces at various machining conditions. This paper introduces a case study on the structural dynamic analysis and test of a 5-axis large scale MTMT in its development stage. The MTMT consists of a ram head module, bed and column as shown in Fig. 2.

In case of insufficient structural stiffness, the machine tool may experience severe vibrations or chatter when it is operating. Consequently the machining accuracy will decrease. It is already known that the machine tool chatter, that is the most troublesome vibration arising in machine tools, is strongly depends on dynamic compliance of the machine tool structure, which is the reciprocal of dynamic stiffness<sup>(4-6)</sup>.

For the purpose of checking up the dynamic characteristics and dynamic compliance of the MTMT proper, we analyzed and evaluated the structural dynamic characteristics, that is, natural frequencies and corresponding mode shapes of the ram head module of the 5-axis MTMT tool by using both F.E.M. and the impulse hammer test. Furthermore, the dynamic compliance of the ram module was also analyzed and measured by using FEM and random excitation test with a hydraulic exciter respectively.

## 2. Modal Analysis

### 2.1 Theoretical modal analysis (by FEM)

Supposing a structure was modeled as a multi-degree of freedom system with structural damping, its equations of motion can be represented as follows

$$[m]\{\ddot{x}\} + [k]\{\dot{x}\} + i[h]\{x\} = \{0\} \quad (1)$$

where  $[m]$ ,  $[k]$ , and  $[h]$  are mass, stiffness, and structural damping matrices, respectively.

Substituting the trial solution  $\{x\} = \{X\}e^{i\omega t}$  into this equation yields following eigenvalue problem.

$$[(k+i[h])-\omega^2[m]]\{X\}=\{0\} \quad (2)$$

For which the non-trivial solutions exist if only the following eigenvalue equation is satisfied.

$$\det[B(\omega)]=\det[(k+i[h])-\omega^2[m]]=0 \quad (3)$$

Typically the structural damping matrix  $[h]$  is proportional.

$$[h]=\beta[k]+\gamma[m] \quad (4)$$

where  $\beta$  and  $\gamma$  are proportional constants. It is clear the eigenvector of this case is the same as that of undamped system.

Then we can determine the complex eigenvalues from Eq. (3).

$$\lambda_r^2 = \omega_r^2(1+i\eta_r) ; \omega_r^2 = \frac{k_r}{m_r} ; \eta_r = \beta + \frac{\gamma}{\omega_r^2} \quad (5)$$

where  $\lambda_r$ ,  $\omega_r$ , and  $\eta_r$  are the complex eigenvalue, the undamped natural frequency, and the damping loss factor for the  $r$ -th mode, respectively.

Substituting this eigenvalue into the Eq. (1) yields a corresponding eigenvector  $\{\phi\}_r$ , which is identical to that of the undamped system.

Since the eigenvector and eigen matrix satisfy orthogonality properties, following relations come out.

$$\{\phi\}_r^T [m] \{\phi\}_r = m_r \quad (6)$$

$$\{\phi\}_r^T [k] \{\phi\}_r = k_r \quad (7)$$

To solve the eigenvalue problem numerically, the Jacobi and Subspace iteration method have been used in this study.

We established a FEM model consisting of 17,976 nodes and 18,832 shell elements to analyze the vibration modes and the dynamic stiffness of the 5-axis MTMT as

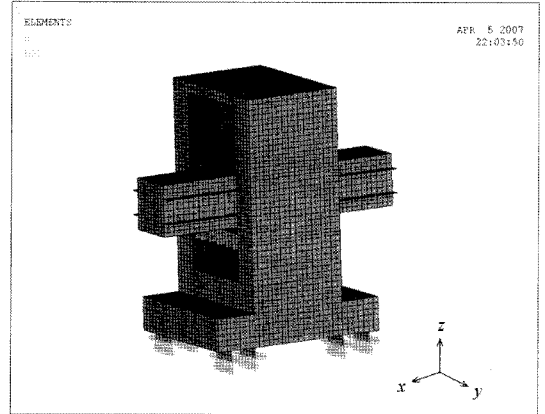


Fig. 3 FEM Model of the 5-axis MTMT

Table 1 FEM modeling data

Element type		SHELL 181
No. of nodes		17,976
No. of elements		18,832
Boundary conditions		Fixed all nodes at 8 LM block
Material constants	Young's modulus, $E$ [GPa]	210
	Poisson' ratio, $\nu$	0.3
	Density [ $kg/m^3$ ]	7,833

shown in following Fig. 3. And the modeling data are listed in Table 1.

## 2.2 Experimental modal analysis (by impulse test)

Fig. 4 represents modal test setup using impulse hammer. According to SISO (Single Input & Single Output) method, an accelerometer is attached to the fixed measuring point of ram head module and we applied impact force to excitation points on the ram head module. The output signal of the measured acceleration is conveyed to FFT analyzer. After obtaining frequency response function about each exciting point, the natural frequencies of the object is measured.

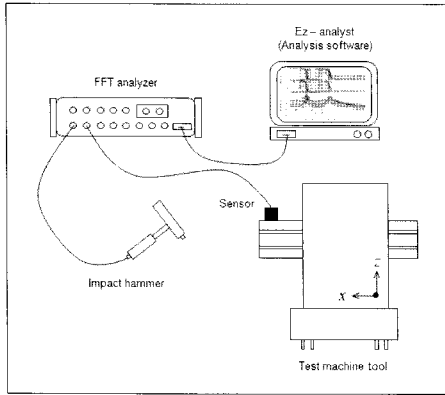


Fig. 4 Illustration of modal test setup

Table 2 Natural frequency of ram head module

Mode No.	Natural frequency [Hz]	
	By FEM	By experiment
1 <sup>st</sup>	59.51	53.75
2 <sup>nd</sup>	83.16	87.81
3 <sup>rd</sup>	92.64	96.88
4 <sup>th</sup>	107.06	116.9

### 2.3 Comparison of modal analysis results

Measured and theoretically analyzed natural frequencies are listed in Table 2 and corresponding mode shapes are compared through Fig. 5 to Fig. 8.

The 1<sup>st</sup> and the 2<sup>nd</sup> modes are the 1<sup>st</sup> bending modes in the Y and Z directions respectively.

The 3<sup>rd</sup> and the 4<sup>th</sup> mode are the 2<sup>nd</sup> bending modes of Z and Y directions respectively.

The 5-axis MTMT, in this paper, has a operating speed of less than 3,000rpm, while the 1<sup>st</sup> natural frequency of ram head module appears over 50Hz. That is the lowest natural frequency is higher than 1X frequency of the maximum operating speed.

## 3. Dynamic Compliance Measurement

### 3.1 Theory of dynamic compliance

In case of forced vibration under harmonic force, the equation follows as Eq. (8).

$$([k] + i[h] - \omega^2[m])\{X\} = \{F\} \quad (8)$$

Where,  $\{F\}$  is excitation force matrix.

Using a system matrix, the displacement matrix of Eq. (8) can be expressed as

$$\{X\} = [B(\omega)]^{-1}\{F\} \quad (9)$$

or

$$\{X\} = [H(\omega)]\{F\} \quad (10)$$

where,  $[H(\omega)]$  is the transfer function, which is the inverse matrix of the system matrix.

$$[H(\omega)] = [B(\omega)]^{-1} = \frac{adj[B(\omega)]}{\det[B(\omega)]} \quad (11)$$

If  $\det[B(\omega)]$  is zero, it becomes characteristic equation. Using the orthogonality of Eqs. (6) and (7), the frequency response function can be written as

$$[H(\omega)] = [\phi] \left[ \frac{1}{m_r(\omega_r)^2 - \omega^2 + i\eta_r\omega_r^2} \right] [\phi]^r \quad (12)$$

When arranging Eq. (12), the frequency response function can be shown as

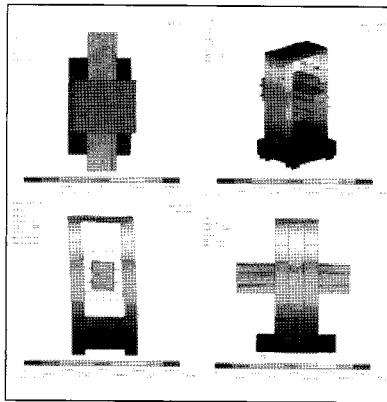
$$h_{ij}(\omega) = \sum_{r=1}^N \frac{{}_r\phi_i{}_r\phi_j}{m_r(\omega_r^2 - \omega^2 + i\eta_r\omega_r^2)} = \sum_{r=1}^N \frac{{}_rA_{ij}}{\omega_r^2(1 + i\eta_r) - \omega^2} \quad (13)$$

where,  $N$  is the rank of matrix,  $m_r$  is the  $r$ -th modal mass,  $\omega_r$  is the  $r$ -th natural frequency, and  $\eta_r$  is the loss factor of the  $r$ -th mode.

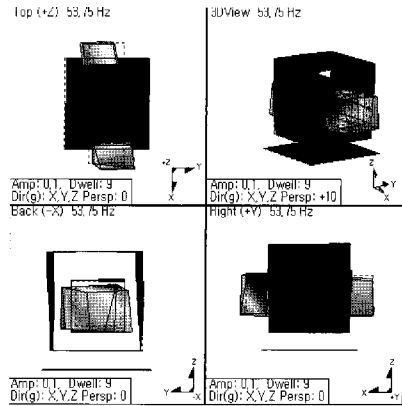
${}_r\phi_i$  and  ${}_r\phi_j$  are respectively the ingredients of the  $r$ -th mode vector and  ${}_rA_{ij}$  is the modal constant or residue.

Transfer function is given by reciprocal of stiffness which is called to compliance,  $G(\omega)$ .

Because it is usually impossible to measure force against displacement to obtain the dynamic stiffness of the machine tool in frequency domain, it can be obtained by measuring displacement against force using the concept of compliance.

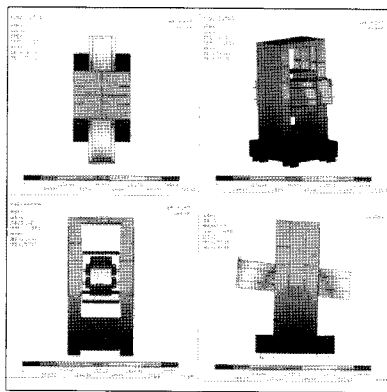


(a) FEM

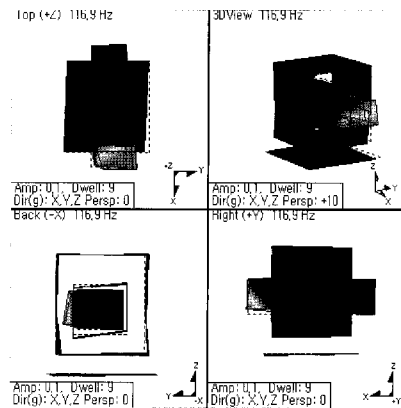


(b) Experiment

Fig. 5 The 1st mode

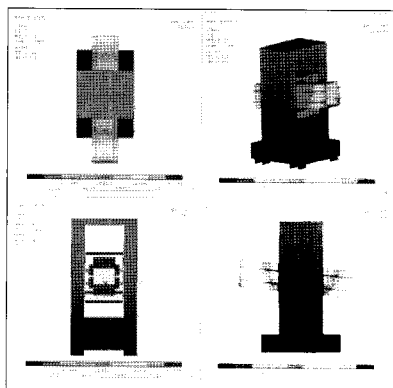


(a) FEM

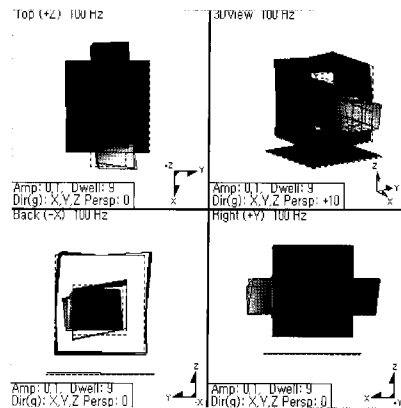


(b) Experiment

Fig. 6 The 2nd mode



(a) FEM



(b) Experiment

Fig. 7 The 3rd mode

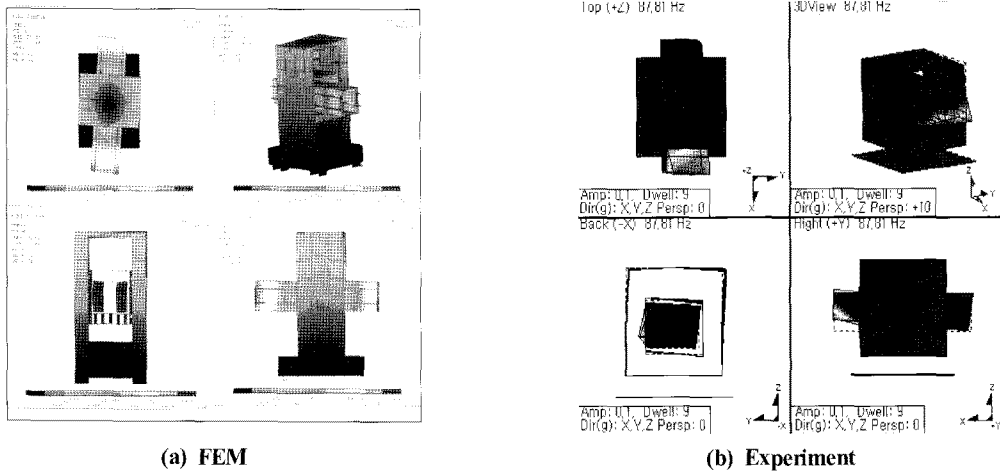


Fig. 8 The 4th mode

Compliance can appear as  $G_{ij}$  according to the direction of exciting force and the measuring direction of displacement. The subscript  $i$  and  $j$  mean the directions of exciting force and the measured corresponding displacement respectively. Since the cutting force exerted on the machine tool has three directional component vectors in the  $x$ ,  $y$ , and  $z$  direction, the resulting displacement may also generated in the three directions.

Thus compliance matrix can express by correlation between exciting forces and the resulting displacement response as follows

$$\begin{Bmatrix} x \\ y \\ z \end{Bmatrix} = \begin{bmatrix} G_{x,x} & G_{y,x} & G_{z,x} \\ G_{x,y} & G_{y,y} & G_{z,y} \\ G_{x,z} & G_{y,z} & G_{z,z} \end{bmatrix} \begin{Bmatrix} F_x \\ F_y \\ F_z \end{Bmatrix} \quad (14)$$

### 3.2 Measurement setup

Fig. 9 shows the test setup for measuring structural dynamic compliance of the MTMT. Exciting force was applied to the ram head end through a hydraulic exciter and the resulting acceleration level was measured on the tool position of the ram head in each X, Y and Z directions respectively.

### 3.3 Comparison of analytical & measured results

Table 3 represents the comparison of the computed and measured structural compliance.

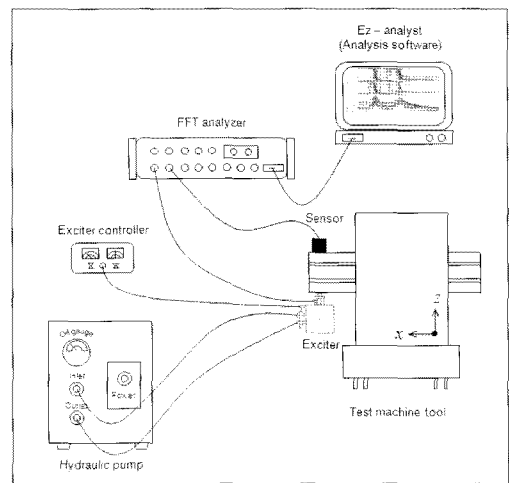
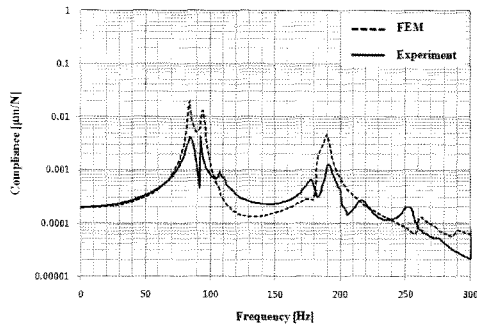
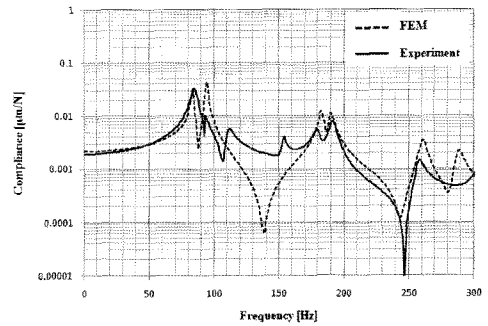
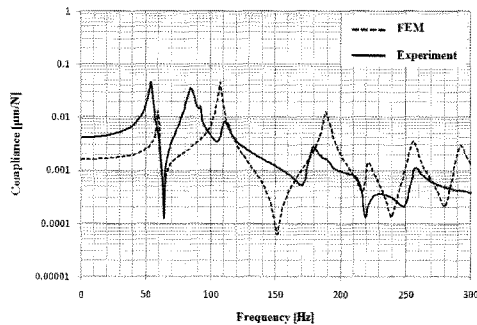
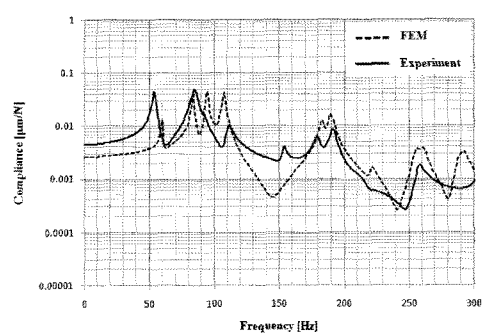


Fig. 9 Dynamic stiffness measurement setup

Table 3 Comparison of structural compliances of MTMT

Direction	Compliance [ $\times 10^{-3}$ $\mu\text{m}/\text{N}$ ]			
	Static		Dynamic	
	Test	FEM	Test	FEM
In x-axis	0.199	0.194	4.36	19.5
In y-axis	1.92	2.17	32.8	44.2
In z-axis	4.11	1.58	38.9	44.9
iso-axial	4.55	2.69	48.5	46.2

(a) The *x*-axial compliance(b) The *y*-axial compliance(c) The *z*-axial compliance

(d) The iso-axial compliance

**Fig. 10 Comparison of the measured and computed compliances of the MTMT**

In Fig. 10, structural compliance response functions obtained from hydraulic exciter test and FEM analysis are well compared in graphic.

#### 4. Concluding Remarks

The findings and results from this case study on the development of a 5-axis MTMT are as follows:

- (1) Measured and calculated natural frequencies of the MTMT showed good agreement with each other and the maximum error between them was less than 10%. Furthermore, the lowest natural frequency was higher than the 1X Hz of the maximum operating speed of the MTMT. Therefore it seems to be rare possibility of resonant bending vibration or modal chatter vibration within operating speed range.
- (2) Measured static stiffness of the MTMT in the

iso-axial direction was  $220\text{ N}/\mu\text{m}$ , while computed one was  $334\text{ N}/\mu\text{m}$ . This indicates that the static stiffness of the developed large scale MTMT has relatively higher stiffness than ordinary medium scale machine tools, whose values are about  $80\sim 100\text{ N}/\mu\text{m}$ . Moreover, the dynamic stiffness in the same direction was measured as  $21\text{ N}/\mu\text{m}$ , and computed as  $22\text{ N}/\mu\text{m}$ , which is also higher than ordinary machine tools.

#### Acknowledgement

This research has been carried out as a part of the R&D project for Local Centric Industrial and Technology Development of the Ministry of Commerce. It has been also financially supported by HNK Machine Tool Co., Ltd. (Grant No. 10017775)

## References

- (1) Choi, Y. H., Jang, S. H., Park, H. M., Jang, S. J., and Cho, Y. J., 2005, "A Genetic Algorithm Based Multi-step Design Optimization of a Machine Structure for Minimum Weight and Compliance," *Proc. of SICE 2005*, pp. 476~481.
- (2) Choi, Y. H., Jang, S. H., Kim, I. S., Cho, Y. J., and Oh, C. W., 2006, "Structural Design Optimization of Multi-tasking Machine with 5-Axes," *Proc. of Korean Society of Machine Tool Engineer Conference*, pp. 215~220.
- (3) Kim, S. G., Jang, S. H., Hwang, H. Y., Choi, Y. H., and Ha, J. S., 2004, "Analysis of Dynamic Characteristics and Evaluation of Dynamic Stiffness of a 5-Axis Multi-tasking Machine Tool by using F.E.M and Exciter Test," *Proc. of ICSMA*, pp. 565~569.
- (4) Tobias, S. A., 1965, *Machine Tool Vibrations*, Wiley, New York.
- (5) Koenigsberger, F. and Tlustý, J., 1970, *Machine Tool Structure*, Pergamon Press, Oxford.
- (6) Weck, M. and Teipel, K., 1984, *Handbook of Machine Tools*, Wiley, New York.
- (7) Ewins, D. J., 1986, *Modal Testing: Theory, Practice and Application*, Research Studies Press, London, pp. 49~64.
- (8) Weck, M. and Eckstein, R., 1987, "An Examination Technique to Determine Static Weakpoints of Machine Tools," *Annals of the CIRP*, Vol. 36, No.1, pp. 257~261.
- (9) Xu, M. and Birchmeier, J. R., 1977, "Dynamic Stiffness Testing and its Applications in Machine Tool," *Journal of Sound and Vibration*, Vol. 31, pp. 8~21.
- (10) Eun, I. U., 2000, "Development of Static and Dynamic Behavior of Machine Tools in the Period from 1980~1990," *Handout of RRC Seminar in Changwon National University*.